Algorithm for Efficient 3D Reconstruction of Outdoor Environments Using Mobile Robots

Jaime Pulido Fentanes*, Eduardo Zalama**, Jaime Gómez-García-Bermejo**,
*CARTIF Foundation, **Instituto Tecnologías de la Producción (ITAP), Universidad de Valladolid

***Abstract* — In this paper, an algorithm for the reconstruction of an outdoor environment using a mobile robot is presented. The focus of this algorithm is making the mapping process efficient by capturing the greatest amount of information on every scan, ensuring at the same time that the overall quality of the resulting 3D model of the environment complies with the specified standards. With respect to existing approaches, the proposed approach is an innovation since there are very few information based methods for outdoor reconstruction that use resulting model quality and trajectory cost estimation as criteria for view planning.**

I. INTRODUCTION

3D modelling of large environments has become a matter of increasing interest in recent years due to its multiple application fields, such as reverse architecture, archaeology, public works or multimedia presentations, among others. This is possible thanks to recent advances in laser scanning technology and related 3D processing algorithms. Laser devices permit automatic scanning of the environment to the desired resolution and measure the geometric coordinates (x,y,z) of every point travelled across by the laser beam, with respect to the scanner location.

However, setting up a typical stationary laser scanning scheme is a difficult and time consuming labour. These devices are usually heavy and require the set up of many different pieces of equipment (tripod, batteries, GPS antenna and computer). Moreover, a human operator has to choose which views will be less occluded and will provide more information and has to decide when the number of scans is large enough to cover the complete model. All this is done usually upon operator experience, without taking a close look at the resulting model.

The use of mobile robots equipped with on board 3D scanning systems emerges as a suitable alternative, ([1], [2], [3]) given that robots provide mobility, computing system, physical support to the scanner and positioning sensors. However, though the use of mobile robots reduces greatly the effort involved in the scanning process, the automation of the view selection is still an open problem.

This issue has been addressed within the field of mobile robot exploration. Most research effort has been focussed on the SLAM (Simultaneous Localization and Mapping) problem, and the developed techniques are designed to improve relevant feature extraction along robot trajectories in order to maximize robot localizability and map information. Usually, the main objective of these approaches is to obtain indoor maps which help robots to self localise, and mapping process is reduced to the x-y dimensions.

Outdoor environments have many characteristics that make the problem different form indoor case. The environment is less structured: it is not restricted by walls, the floor is not plain, there are arbitrary but relevant 3D elements (such as trees, stones and cars), and thus 2D maps are not efficient for navigation purposes. Moreover, 3D mapping is a more complex problem due the huge memory and computational resources required for data handling, besides of other problems such as occlusions. Fortunately, the localization problem is less severe in outdoor environments due the availability of absolute localization sensors like DGPS and compasses, which provide reasonably accurate robot localization.

Under these circumstances, the algorithm presented in this paper is focused on optimizing the exploration process by maximizing the map quality, while reducing the amount of scans required for creating a good quality 3D model of the environment. The goal is to have a robot that can build a model of its surrounding environment in an efficient way, so this robot has to consider previous data to choose the best next locations to carry out a new scan, and compute the trajectory towards these locations. This methodology can be applied to most outdoors scenes such as urban locations, monuments, archaeological sites and forest.

II. PREVIOUS WORK

Several exploration techniques have been proposed in the literature, following two main strategies: strategies where a given trajectory or behaviour (e.g. wall following or moving to random positions) is defined upon a priori information of the environment ([4], [5]), and strategies that *predict* which movement will improve the most the robot knowledge of the environment, based on acquired information.

The first group of strategies lacks adaptability to unknown environment, where they tend to either leave unexplored areas or be highly inefficient. Therefore, the second group of strategies has received more attention since environment information is used to decide further actions and they are more adaptable to any kind of environment. In general methods belonging to this second group are known as ***next best view*** (***nbv***) given that their focus is to find the best next observation position.

Common methods within ***nbv*** approaches are greedy methods [6], where the robot moves to the closest location of interest; frontier based methods [7], where candidate

---

This research has been supported by the Science and Innovation Spanish ministry (Pr. Nb.DPI2008-06738-C02-01/DPI), and the Consejería de Educación of the Junta de Castilla y León (Pr. Nb. VA001A10-2).
The first author is with CARTIF Centro Tecnológico, Dep. Of Robotics and Computer Vision, Boecillo (Valladolid, Spain); email: { jaipul@cartif.es }.
The second and third authors are with the University of Valladolid (Spain), Dep. Of Systems Engineering and Automatic Control, Industrial Engineering School; email: {ezalama@eis.uva.es, jaigom@cartif.es }

locations are generated on the frontier between the explored and unexplored areas; and information based strategies that use evaluation functions where different criteria is employed to choose the next best position according to the selected criteria, for example *traveling cost* [8].

Among the information based works, some of them use functions to predict the utility of a given location. For example, in [9] the utility of a target location is defined as an expected information gain. In [10] traveling cost is combined with *information gain* so that the next best view point is chosen to maximize coverage and reduce traveling distance. Some strategies find *interest areas* within the map that are also used as a criteria, for example in [11] relevant features within the map are included and used for evaluating next best view considering that seeing these *regions* will facilitate SLAM.

For 3D mapping, [12] proposes a hierarchical ***nbv*** method for quickly evaluating multiple 3D views in indoor scenarios using model quality and completeness as criteria, this work presents different algorithms to efficiently evaluate several viewpoints with respect to large sets of 3D data where different where positioning and sensing constraints are taken into account. A different solution for outdoor 3D mapping is proposed in [13], where a 2D floor map of the area to be scanned is used to find possible occlusions that a 3D scan would have from different floor points. The combination of viewpoints that requires the lowest number of scans to entirely cover the target area is then found upon this process. Once a 3D scan has been taken from each previously calculated viewpoint, a view planning algorithm is used to cover all unpredicted occlusions on the model with as few scans as possible.

III. The Experimental Framework

The proposed algorithm has been designed for an all-terrain robot we have developed for outdoor 3D reconstruction (Fig. 1). This robot has a six wheel differential traction system, an electronic traction control system, an on-board PC system, and a multi-channel, long-range communication system for teleoperating or monitoring the robot in autonomous and semi-autonomous missions, as well as different navigation sensors (cameras, laser, GPS and IMU).

Fig. 1: All-terrain Robot developed by CARTIF

The robot is also provided with an on-board 3D scanner (Fig. 2) designed within this work. It uses a 2D Sick LMS-111 laser system on a rotating platform that spins at a 0.2 to 5 hz speed. The scan resolution of this system depends on the spinning speed and the number of turns of the scanner. A typical scan has a 0.5º x 0.5º pant-tilt resolution and takes about 10 seconds to be completed.

However, given that the development of an exploration algorithm requires extensive tests and the scanning of different environments from as many viewpoints as possible, simulation becomes desirable and is a better suited tool for the development of the algorithm.

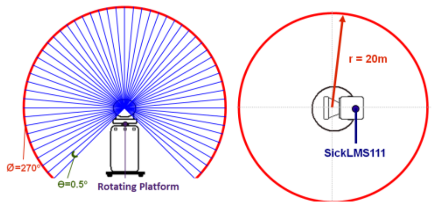

Fig. 2: Representation of a laser scan: front view (left) and top view (right). SickLMS-111 mounted on a spinning platform allows obtaining an almost full environment scanning coverage.

Therefore, we have developed a 3D robotic environment simulator (Fig. 3), that simulates our robotic system on which exploration algorithm tests can be run at a low cost. The simulator has been developed in C++ using ODE dynamic simulation libraries [14] for the simulation of physic variables and ray collider. 3D data loading has been implemented using Trimesh2 [15] libraries. IPC [16] libraries have been used for communicating simulator with other programs such as the proposed exploration algorithm. This way, transition from simulated environments to real scenarios is quick and transparent to the user. The simulator is open software that can be downloaded from https://sourceforge.net/projects/simbot3d, and future releases will include communication with well-known *Player-Stage* [17].

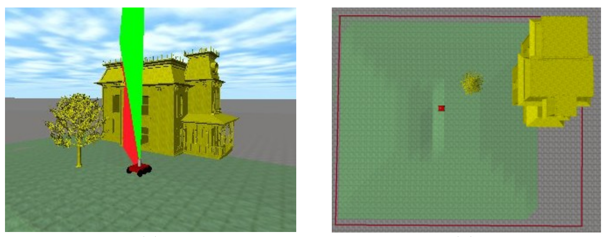

(a) (b)

Fig. 3: Simple environment simulation screenshot. Frontal Camera (a) and aerial view (b).

IV. Overview Of The Proposed Algorithm

The proposed method is based on the multiple criteria ***nbv*** algorithm [18], where not only the distance and the expected information gain is considered for exploration, but also other critical information such as resulting model quality, view occlusion and navigation difficulty,

$$u(t) = \frac{w_A A(t)\cdot w_Q Q(t)\cdot w_O O(t)}{w_C C(t)} \qquad (1)$$

In this equation, *u(t)* is the utility evaluation function used by the algorithm, *t* is the candidate position to be evaluated, *A(t)* is a normalized value that represents expected information gain, *Q(t)* is the improvement on model quality, *O(t)* stands for the number and quality of interest zones covered from target *t*, *C(t)* is a cost function that quantifies the difficulty of reaching each target; and w_A, w_Q, w_O and w_C are constant values that weight the influence of each criteria in the evaluation function.

All these criteria are chosen in order to obtain an environmental 3D model that fulfils model quality requirements while reducing the number of scans needed to cover the working area during movement, thus reducing the process time and energy requirements.

Figure 4 shows the flowchart of the proposed algorithm, Input information is the scanned point cloud data, and an OpenGL Style transformation matrix which represents the robot pose. A 3D analysis process is carried out in order to determine robot navigation area, model quality analysis and interest zone extraction. Afterwards a 2D grid map is created to calculate information about the resulting model quality and robot navigability, and over which a set of candidate targets is created. Finally, each created target is evaluated using the utility evaluation function to determine from where the next scan should be taken.

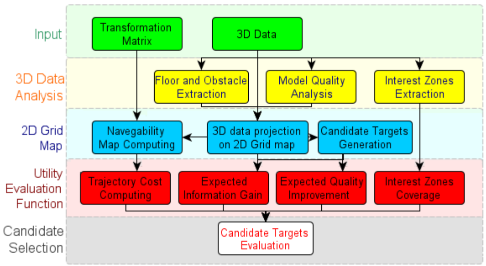

Fig. 4: Algorithm block diagram

V. 3D DATA ANALYSIS

In this stage, the acquired 3D mesh is analyzed point by point in order to extract which points correspond to traversable surfaces and obstacles, to estimate model quality at each point and to extract interest zones from discarded triangles. This process is executed every robot scan.

A. Extraction of Safe Navigation Zones and Obstacles

3D data contains a large amount of information about the environment, and 3D points can correspond to obstacles, drivable surfaces (ground) or objects that the robot cannot reach [19]. The extraction of safe navigation areas is done by calculating the probability of each point of the mesh of belonging to the ground (safe navigation zones) or an obstacle. This data is useful to analyze navigability within the surrounding area.

If a point is at a reachable angle for the robot (i.e. the robot does not need to climb beyond its possibilities to reach this point), and its normal vector projection onto the world Z axis has is large enough, this point has a high probability of belonging to a traversable zone from a *local* point of view.

However, neighboring points have to be also considered, for example, a point on an elevated plane may comply with *local* conditions, but its neighbor probabilities could be largely lower.

For this reason, the extraction of safe navigation areas is done in two steps. First, a probability from a local point of view $F_{pl}(p)$ is computed using (2), where *Pz* is the point height, *dp* is its distance to the scanner on the XY plane, *Nz* is its normal Z component on the global reference system and Θ is the maximum angle that the robot can climb.

$$F_{pl}(p) = |N_z| \cdot \left(1 - \frac{P_z}{d_p \sin(\theta)}\right) \quad (2)$$

Then, a probability from a "global" point of view $F_{pg}(p)$ is computed as the average of each neighboring point probability, $F_{pl}(p)$ (points sharing 3D mesh triangles with point *p*),

$$F_{pg}(p) = \frac{1}{n} \sum_{i \in \gamma(p)} F_{pl}(i) \qquad (3)$$

where *γ(p)* is the set of neighbors of point *p* and *n* is the number of neighbors. Once $F_{pg}(p)$ has been computed, the final probability *F(p)* for each point is obtained by weighting w_l and w_g their corresponding probabilities,

$$F(p) = w_l F_{pl}(p) + w_g F_{pg}(p) \qquad (4)$$

A point can belong to an obstacle if it is at a reachable position for the robot and the plane to which it belongs to is facing the robot (the dot product between the ray and the point normal vector is close to 1). Neighbours are also important since an obstacle point surrounded by floor points can be traversable. The probability of belonging to an obstacle is computed using a "local" probability function $B_l(p)$ (5) and a "global" probability function $B_g(p)$ (6):

$$B_l(p) = |N_{xy}| \left(\frac{\vec{P}}{|P|} \cdot \vec{N}\right) \quad (5)$$

$$B_g(p) = \frac{1}{n} \sum_{i \in \gamma(p)} B_l(i) \quad (6)$$

where $|N_{xy}|$ is the magnitude of the resulting vector addition of point normal components on X and Y axis, $\vec{\boldsymbol{P}}$ is a vector from the 3D scanner to point *p* and $\vec{\boldsymbol{N}}$ is its normal vector. In (6), the neighbours to point *p* are used to find the global probability value. Then, the final probability *B(p)* is obtained by weighting with w_{bl} and w_{bg} the $B_l(p)$ and $B_g(p)$ relevance,

$$B(p) = w_{bl} B_l(p) + w_{bg} B_g(p) \quad (7)$$

Some results can be seen in Fig. 5. Ground and obstacle probability values are used to create a navigation map that is used to find trajectories and calculate route difficulty, as will be explained in section VI.

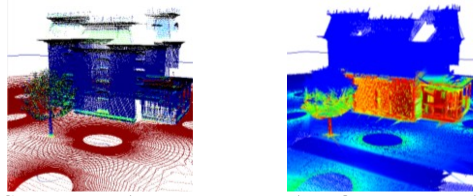

Fig. 5: Left: Ground Extraction Process Result. Right: Obstacle Extraction Result

B. Model Quality Analysis

Model Quality has to be analysed point by point because it is not a homogeneous characteristic and is affected by various factors within one scan. In the analysis process each point *p* gets a score (between 0 and 1) ***AP(p)*** where 0 correspond to bad quality and 1 to the desired quality or better. This score is given according the following criteria,

$$AA(p) = \begin{cases} \left(\frac{A_{max}}{P_{Ar}}\right), & P_{Ar} > A_{max} \\ 1, & P_{Ar} \leq A_{max} \end{cases} \quad (8)$$

$$AI_p(p) = \left(\frac{\vec{P}}{|P|} \cdot \vec{N}\right) \quad (9)$$

$$AP(p) = \frac{\sqrt{[\omega_a AA(p)]^2 + [\omega_n AI_p(p)]^2}}{\sqrt{(\omega_a{}^2 + \omega_n{}^2)}} \quad (10)$$

where *AA(p)* is a function that compares current area per point against maximum desired point area for point p, P_{Ar} is point p area, A_{max} is the desired point area, $AI_p(p)$ is a quality factor that depends on ray incidence angle for point's plane**,** $\vec{P}$ is a vector from the 3D scanner to point p and $\vec{N}$ is its normal vector. Finally, ω_a and ω_n are parameters to adjust area against ray incidence angle relevance. Fig. 6 shows model quality by area and ray incidence angle.

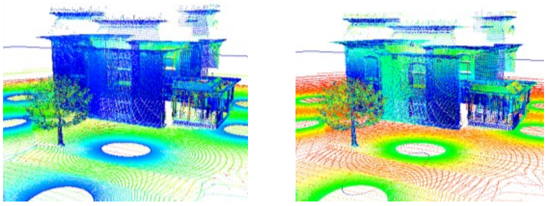

Fig. 6: Left: Map Quality by Point Area criteria. Right: map quality by ray incidence angle criteria (cold colours mean higher quality)

C. Extraction of Interest Zones

The last step in the 3D analysis process is the extraction of the interest zones. These zones are extracted from model discarded triangles, which usually are occluded planes.

In order to be useful for utility evaluation, a vector that points to the centre of each occluded plane is created. These vectors are stored on a list along with points at the centre of each occluded plane, and are used to measure how well interest zones will be scanned from each candidate position.

The resulting list is projected onto the 2D information grid where information on which occlusion planes and how are they covered from each evaluated target *t*, can be extracted using

$$O(p) = \sum_{j \epsilon \delta} \sum_{i \epsilon \beta_j} |\vec{r_e} \cdot \vec{V_i}| \quad (11)$$

δ is the set of visible cells from target *t*, β is the set of interest zones stored for each cell *j*, $\vec{\mathbf{r}}_{\mathbf{e}}$ is a vector from the 3D scanner to the point that marks the centre of an interest zone and $\vec{V}$ is the vector that is normal to the occlusion plane.

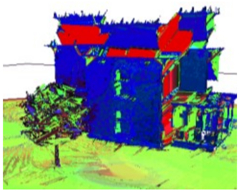

Fig. 7: Interest Zones (in red) Extracted From One Scan

VI. Evaluation of Candidate Targets

Candidate evaluation using 3D data can be a really high resource and time consuming process. For this reason, a 2D information grid is used in this work, in order to keep time and resources low without losing information from 3D data. Each cell in this grid stores all the information from an area of the environment, so processing information becomes much simpler. All the information of a mesh is projected onto the grid every time a new scan is taken.

This representation is useful for many different tasks, such as computing navigation maps by analysing the amount of points that have high probability of belonging to obstacles or traversable surfaces in a cell.

A. 2D Navigation Map

This representation is based on the navigability concept [20]. It is a map very similar in appearance to occupancy grid maps used for 2D environments. However, cells in occupancy maps contain the probability of a cell of being occupied by an object, while cells in the navigation map contain the probability of a cell of being traversable by the robot.

Each time a new point with high probability of belonging to a traversable surface is added to a cell, the probability of this cell to be traversable is increased. Otherwise, if an obstacle point is added, then this probability is decreased. Navigability per cell $C_{nc}(c)$ has ranges from 0 to 1, 1 corresponding to a completely traversable cell. This map (see Fig. 8) is computed using all points that have a probability of belonging to a traversable surface over a given ε_f value, or a probability of belonging to an obstacle over a ε_o value.

$$r_{fo} = \frac{n_{pf}}{n_{pf} + n_{po}} \quad (12)$$

$$F_c(c) = \sum_{i \in \varphi} F(i) \quad (13)$$

$$B_c(c) = \sum_{i \in \alpha} B(i) \quad (14)$$

$$C_{nc}(c) = 0.5 + \left(r_{fo} \frac{n_{pf} F_c(c)}{2}\right) - \left((1 - r_{fo}) \frac{n_{po} B_c(c)}{2}\right) \quad (15)$$

In this expression, φ is the set of points on cell *c* with $F(p) \geq \varepsilon_f$, n_{pf} is the number of points in set φ, $\propto$ is the set of cell points with $B(p) \geq \varepsilon_o$ and n_{po} is the number of points in group $\propto$.

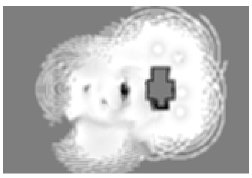

Fig. 8: Navigation Map

Candidate targets are generated in cells where $C_{nc}(c) > 0.6$, so that every evaluated target is reachable. Targets are distributed uniformly around robot position; so many different viewpoints are evaluated.

B. Expected Information Gain

In order to compute how much new information can be captured from each evaluated candidate, the number of points and the minimum and maximum point heights per cell are used. This information is used to compute how many new cells will be scanned from each target and which cells will be occluded by other ones.

The first relevant value is the area covered from each candidate target $A_n(t)$, which is computed using

$$A_n(t) = \frac{A_c C_{se}}{\pi r_e^2} \qquad (16)$$

where Ac is the area represented by each cell and C_{se} is the number of unexplored cells within the scanner range. Computation is refined by subtracting the area of occluded cells $A_o(t)$ from the unexplored area that could be covered from a given candidate target.

Occluded cells are computed using a height map that is created using per cell min and max point height; and using for unexplored cells the info of the closest explored cell in robot direction.

Using map information, three points m_k are generated: one point at the minimum height of each cell, other one at the maximum height that the scanner could reach on that cell from the evaluated target, and another one at the middle of said points. Then, lines are traced from the scanner position at the evaluated target t to each of these three points, and lines that cross a cell under its maximum height n_{il} are counted. The occluded area is then computed using

$$A_o(t) = \frac{n_{il} A_c}{3} \qquad (17)$$

The expected information gain ***A(t)*** can be computed upon (16) and (17) using

$$A(t) = A_n(t) - A_o(t) \qquad (18)$$

C. Expected Model Quality Gain

Model quality gain is the difference between quality information stored in the 2D information map, and the quality information after a scan from the evaluated target t is taken.

Expected quality is calculated using two terms. The first term is expected per cell point area EQ_{AP}, which is computed using the distance from the candidate target to each cell r_e, the maximum desired point area A_{max} and Pan-Tilt resolutions res_p and res_t.

$$PA_c(c) = r_e^2(\sin(res_p)\sin(res_t)) \qquad (19)$$

$$EQ_{AP}(c) = \begin{cases} \frac{A_{max}}{PA_c(c)}, & PA_c(c) \geq A_{max} \\ 1, & PA_c(c) < A_{max} \end{cases} \qquad (20)$$

The second term corresponds to the quality improvement computed from laser incidence angle. A new ray incidence quality for each point on the cells that are within the scanner reach from the evaluated target, $EI_C(c)$, is computed using

$$EI_c(c) = \frac{1}{np_c} \sum_{k \in \varphi} \left(\frac{\overrightarrow{R_k}}{|R_k|} \cdot \overrightarrow{N_k} \right) \qquad (21)$$

where φ is the set of points stored in each cell, n_{pc} is the number of points in each cell, $\overrightarrow{\boldsymbol{R}}$ is a vector from the evaluated target to each cell point and $\overrightarrow{\boldsymbol{N}}$ is a unit vector normal direction to each cell point. Expected quality gain $Q(t)$ is obtained using

$$Q(t) = \sum_{c \in \sigma} \left(\frac{\sqrt{[\omega_a EQ_{AP}(c)]^2 + [\omega_n EI_c(c)]^2}}{\sqrt{(\omega_a{}^2 + \omega_n{}^2)}} - \frac{1}{np_c} \sum_{p \in \varphi} AP(p) \right) \qquad (22)$$

where σ is the set of cells within the range of the scanner, $AP(p)$ is the quality per point mark computed in section V-B, and ω_a and ω_n are the values introduced in that section.

D. Trajectory Cost Evaluation

Trajectory cost evaluation is done by adding the difficulty of crossing each cell on the trajectory. This difficulty depends on the slope of each cell, the difference between the entry and the exit angle for each cell, the navigability $C_{nc}(c)$ value computed in section VI-A and the distance between cells d_{ec}. It is computed using:

$$C_c(c) = d_{ec} \frac{f_{ga}\left(\frac{hmin_{ci} - hmin_{ci+1}}{\sin^{-1}(\theta_{max})}\right)}{C_{nc}(c)} \qquad (23)$$

where f_{ga} is a difficulty scale factor that depends on the trajectory curvature (see Fig. 9), ci is the current cell in the trajectory and Θ_{max} is the maximum slope that the robot can climb.

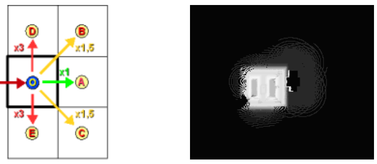

Fig. 9: Left: difficulty factor when crossing Cells; Right: Difficulty Map upon Slope

VII. Results

Four experiments carried out on a simple environment in the simulator (see section III) are shown for evaluating the proposed algorithm, the first three experiments are done using the proposed algorithm, the fourth experiment is an implementation of a greedy mapping algorithm for comparison purposes. The area to be explored is shown in figure 3b. Three different value choices for parameters in (1) were tested in order to achieve different objectives. In the first experiment, the parameters have been set in an equilibrate way; in the second experiment information gain has been given more importance than the other parameters; and in the third experiment, model quality has been the dominant criteria. The parameter values chosen for the first three experiments can be seen in Table I.

TABLE I
PARAMETERS USED IN THE THREE EXPERIMENTS

	w_A	w_Q	w_O	w_C
Experim. I	0.43	0.35	0.22	0.09
Experim. II	0.65	0.25	0.10	0.09
Experim. III	0.36	0.5	0.14	0.09

In all experiments, A_{max} was 0.025m^2 and 2D cell size was 0.3m x 0.3m. w_c parameter was not modified so trajectories were determined only by the desired model criteria. The amount of targets evaluated after each scan varies depending on the number of traversable cells with a maximum of 1/25th of those cells. Resulting trajectories can be seen in Fig. 10.

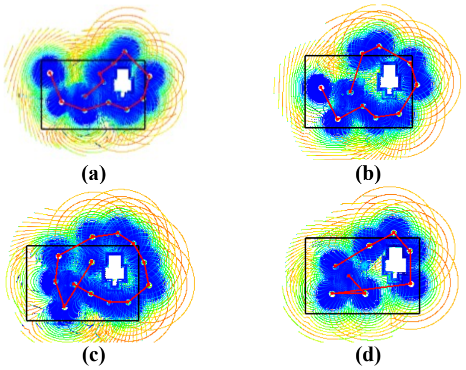

Fig. 10: Resulting trajectories for Exp. I (a); Exp. II (b); Exp. III (c); Exp. IV(d). Colder Colours Represent Better Quality

Table II shows the result for each experiment in terms of travelled distance, the number of scans done in each experiment, the amount of cells explored within the given area and a quality score given by the mean of per point quality score on each cell within the area to be explored.

TABLE II
RESULTS OBTAINED IN EXPERIMENTS

	Travel Distance	Quality Score	Coverage	Scans
Experim. I	106 m	0.6846	92.5 %	12
Experim. II	107 m	0.6904	94.1 %	10
Experim. III	128 m	0.7503	93.6 %	13
Experim. IV	116 m	0.5013	91.4 %	8

All experiments were stopped when the coverage was over 90% of the reachable cells. Experiment II proved to be the most efficient one since it covered the entire area using only ten scans whilst travelling only 1 meter more than the shortest trajectory. On the other hand, Experiment I provided a very similar model but took two extra scans. Experiment III required more scans (13) than any other test and more travel distance than any other test; however it captured a very high quality model.

Experiment IV showed that, in comparison with the greedy mapping algorithm, the proposed algorithm may require more scans to achieve the same level of coverage. However, it leads to much higher quality score. The difference in terms of traveled distance and coverage is not noticeable, but trajectory is inefficient for greedy method since it requires the robot to execute rougher turns for reaching the targets. Finally, there is an important difference in the quality distribution, this distribution being much more uniform in the experiments carried out with the proposed algorithm, as can be seen in Fig. 10.

Algorithm execution times vary greatly depending on the amount of 3D data to be processed, however for these experiments on a 3GHz Intel Core2 Duo processor the 3D analysis process took around 350 ms each time a new scan was made, and for the target evaluation step the evaluation time for each target was at most 100 ms.

VIII. CONCLUSION

An algorithm for efficiently planning of viewpoints from 3D data, for 3D reconstruction of outdoor environments, has been presented. Different criteria are used by this algorithm, in order to obtain a model with quality over a predefined minimum. The trajectory that the robot must follow in order to reach each possible target is also considered, so the process is carried out keeping a balance between the utility of a point and the cost of getting to it.

The way the 3D data are processed in order to quantify the model quality and extract navigation surfaces, obstacles and interest regions has been discussed. Also a navigation map useful for 3D environments and its resemblance to 2D occupancy grid maps has been introduced.

The obtained results show that the algorithm can calculate efficient trajectories for reconstructing the environment, and that these trajectories change depending on the parameters chosen to fulfill a given criterion. Also, our preliminary tests of the algorithm implemented on the real robot (see Fig. 1) have led to similar results than those obtained in simulation. These results will be presented in future publications.

REFERENCES

[1] P. Blaer and P. Allen, “Data Acquisition and View Planning for 3-D Modeling Tasks”. In IROS2007, San Diego, 2007.
[2] A. Nuchter, K. Lingemann, and J. Hertzberg. “Extracting drivable surfaces in outdoor 6d slam”. In the 37nd Symp. on Robotics (ISR ’06), Munich, 2006.
[3] A. Nüchter, “3D Robotic Mapping”, Springer
[4] E. Bourque and G. Dudek, “Viewpoint selection-an autonomous robotic system for virtual environment creation,” in IROS98, vol. 1, 1998,
[5] T. Danner and L. E. Kavraki, “Randomized Planning for Short Inspection Paths,” Proceedings of IEEE International Conference on Robotics and Automation ICRA '00. 2000.
[6] Tovey, C.; Koenig, S.; “Improved Analysis of Greedy Mapping”, Proceedings of IEEE/RSJ International Conference on Intelligent Robots and Systems, (IROS 2003). 2003.
[7] B. Yamauchi, “A frontier-based approach for autonomous exploration,” in Proceedings of the IEEE International Symposium on Computational Intelligence in Robotics and Automation, July 1997, pp. 146–151.
[8] B. Yamauchi, A. Schultz, W. Adams, and K. Graves, “Integrating map learning, localization and planning in a mobile robot,” in Intelligent Control (ISIC), 1998.
[9] P. Newman, M. Bosse, and J. Leonard, “Autonomous feature-based exploration,” in the IEEE International Conference on Robotics and Automation, 2003.
[10] H. H. Gonzalez-Baños and J. C. Latombe, “Navigation strategies for exploring indoor environments.” International Journal of Robotics Research, vol. 21, pp. 829–848, 2002.
[11] R. Grabowski, P. Khosla, and H. Choset. “Autonomous exploration via regions of interest”. In IEEE IROS, pages 27–31, 2003.
[12] K. Low and A. Lastra, "Efficient Constraint Evaluation Algorithms for Hierarchical Next-Best-View Planning," Third International Symposium on 3D Data Processing, Visualization, and Transmission (3DPVT'06), 2006
[13] P. Blaer and P. Allen, “View Planning and Automated Data Acquisition for Three-Dimensional Modeling of Complex Sites”, Journal of Field Robotics 26(11–12), 865–891 (2009)
[14] R. Smith; “Open Dynamics Engine”, http://www.ode.org/
[15] S. Rusinkiewicz, “trimesh2”, http://www.cs.princeton.edu/gfx/proj/trimesh2/
[16] R. Simmons, “Inter Process Communication”, http://www.cs.cmu.edu/~ipc/
[17] B. Gerkey and R. Vaughman; “The player project”, http://playerstage.sourceforge.net/
[18] N. Basilico and F. Amigoni. “Exploration strategies based on multicriteria decision making for an autonomous mobile robot”. Proc. ECMR09, 2009
[19] A. Nuchter, K. Lingemann, and J. Hertzberg. “Extracting drivable surfaces in outdoor 6d slam”. In Proc. of the 37nd Int. Symp. on Robotics (ISR ’06), Munich, Germany, 2006.
[20] J. Hertzbert, K. Lingemann, C. Lorken, A. Nuchter and S. Stiene. “Does it help a robot navigate to call navigability an affordance?”. Towards affordance-based robot control. In *Lecture Notes in Computer Science* 2008.